



OPEN

Ab initio adiabatic study of the AgH system

Tahani A. Alrebdī¹, Hanen Souissi²✉, Fatemah H. Alkallas¹ & Fatma Aouaini¹

In the framework of the Born–Oppenheimer (BO) method, we illustrate our ab-initio spectroscopic study of the silver hydride molecule. The calculation of 48 electrons for this system is very difficult, so we have been employed a pseudo-potential (P.P) to reduce the big number of electrons to two electrons of valence, which is proposed by Barthelat and Durant. This allowed us to make a configuration interaction (CI). The potential energy curves (PECs) and the spectroscopic constants of AgH have been investigated for Σ^+ , Π and Δ symmetries. We have been determined the permanent and transition dipole moments (PDM and TDM), the vibrational energies levels and their spacing. We compared our results with the available experimental and theoretical results in the literature. We found a good accordance with the experimental and theoretical data that builds a validation of the choice of our approach.

Transition metal hydrides (TMH) play a crucial role in the chemistry due to their potential use from catalysis to energy applications^{1–3}. In this context, many efforts have been carried out understand their spectroscopic, electronic, and structural properties of TMH. Among them, AgH have been studied by Stephen et al.⁴ using large valence basis sets in connective with relativistic effective core potentials (RECPs).

The silver hydride AgH molecule has been the subject of several experimental^{5–11} and theoretical^{4,12–25} works. There is four experimental studies have been examined by Le Roy et al.⁵, Seto et al.⁶, Rolf-Dieter et al.⁷ and Helmut et al.⁸. In addition, this system has been theoretically studied by several works^{4,12–25}. Their works were only limited to the study of the ground state $X^1\Sigma^+$ and the first excited state $A^1\Sigma^+$. We have been performed a study on AgH molecule because of the absence of the characteristic spectroscopic results for the AgH molecule required for the drafting and the realization of many experimental work. Bengtsson and Olsson²⁶ have been determined the first spectroscopic constants for the $A^1\Sigma^+$ and $X^1\Sigma^+$ states by determining the emission spectrum of the $A^1\Sigma^+ - X^1\Sigma^+$ transition.

We have been beginning by determining the curves of adiabatic potential energy of all states (Σ), (Π) and (Δ) symmetries singlets and triplets that are tends to their ionic limit (Ag^+H^-) as well as the constants spectroscopic (well depth D_e , equilibrium distance R_e , transition energy vertical T_e , the anharmonicity constant $\omega_e\chi_e$, the vibration pulsation ω_e and the constant rotational B_e).

Theoretical background

The spectroscopic is a main topic in the theoretical research, which is carried out in our Laboratory of Quantum Physics. We have been performed an ab-initio study of the AgH molecule in the framework of the adiabatic B.O. approximation to determine the ground state $X^1\Sigma^+$ and the other lowest excited states of sigma(Σ^+), pi (Π) and delta(Δ) symmetries.

The silver atom is composed of 47 electrons whose (1s², 2s², 2p⁶, 3s², 3p⁶, 3d¹⁰, 4s², 4p⁶, 4d¹⁰, 5s¹) is the fundamental electronic configuration. This atom is considered as a system with a one valence electron by replacing the core electrons with a proposed pseudo-potential of Barthelat and Durand^{27,28}. Whereas, the hydrogen atom is composed of one electron, when the fundamental electronic configuration is (1s¹). The interaction of the silver core with the electrons valence of hydrogen atom is represented by the core polarization potential (CPP), given by Muller et al.²⁹ and it is given as follows

$$V_{CPP} = -\frac{1}{2} \sum_{\gamma} \alpha_{\gamma} \vec{f}_{\gamma} \vec{f}_{\gamma} \quad (1)$$

\vec{f}_{γ} is the electrostatic field that is at center γ generated through the valence electrons and all the other centers' cores and α_{γ} is the dipole polarizability of the core γ that is given as following.

¹Physics Department, College of Sciences, Princess Nourah Bint Abdulrahman University, P.O Box 84428, Riyadh 11671, Saudi Arabia. ²Laboratoire de Physique Quantique, Faculté des Sciences de Monastir, Université de Monastir, Avenue de l'Environnement 5019, Monastir, Tunisie. ✉email: hanensouissi9@gmail.com

Atomic levels	This work	Experimental ³²	ΔE
5s	-61,106.450	-61,106.450	0.00
5p	-30,940.655	-30,940.655	0.00
6s	-18,553.068	-18,550.298	2.80
6p	-12,639.763	-12,673.446	33.68
5d	-12,350.276	-12,350.331	0.00
7s	-9213.106	-9219.476	6.40
7p	-6985.658	-7012.034	26.40
6d	-6892.600	-6897.060	4.45

Table 1. Theoretical ionization energies (in cm^{-1}) of silver atom compared with the experimental ones³². ΔE Energy difference between the experimental values and theoretical work in cm^{-1} .

Atomic levels	This work	Experimentale ³²	ΔE
1s	-109,725.89982	-109,678.77159	47.12
2s	-27,371.77786	-27,419.81712	48.04
2p	-27,369.80259	-27,419.60862	49.8
3p	-12,189.62067	-12,186.48811	3.13

Table 2. Theoretical ionization energies (in cm^{-1}) of hydrogen atom compared with the experimental ones³². ΔE Energy difference between the experimental values and theoretical work in cm^{-1} .

$$\vec{f}_\gamma = \sum_i \frac{\vec{R}_{\gamma i}}{R_{\gamma i}^3} F_1(R_{\gamma i}, \rho_\gamma^1) - \sum_{\gamma' \neq \gamma} Z_c \frac{\vec{R}_{\gamma' \gamma}}{R_{\gamma' \gamma}^3} \quad (2)$$

$F_1(R_{\gamma i}, \rho_\gamma)$ represents the cut-off function dependent on ρ_γ according to the expression given by Foucault et al.³⁰ in the following form.

$$F(R_{\gamma i}, \rho_\gamma) = \begin{cases} 0; & R_{\gamma i} < \rho_\gamma \\ 1; & R_{\gamma i} > \rho_\gamma \end{cases} \quad (3)$$

where the formulation present the cut-off radius.

$$F(R_{\gamma i}, \rho_\gamma) = \sum_{l=0}^{\infty} \sum_{m=-l}^{+l} F_l(R_{\gamma i}, \rho_\gamma) |lm_\gamma\rangle \langle lm_\gamma|$$

whereas, the operator $|lm_\gamma\rangle \langle lm_\gamma|$ was the spherical harmonic in the center of core γ .

The parameters α_γ and ρ_γ were adjusted to reproduce the experimental ionization potential and the energies of the lowest excited levels. We have been used the core polarizability of the silver is $\alpha_{Ag} = 9.32a_0^{329}$ and $\rho_s = \rho_p = \rho_d$ are the optimized cut-off parameters are equal to 2.00 Bohr.

Results

Basis set. To have a perfect representation of this atomic levels (7s, 7p, 6d, 8s, 8p, 7d, 9s and 9p) of Ag atom, we have been optimized a large Gaussian-Type Orbital (GTO) basis set, which is 8s/6p/5d (see Table 1). While for the hydrogen atom, we have been used this basis (7s/3p/2d), which was re-optimized by the basis set studied by Zrafi et al.³¹ (see Table 2). Therefore, we have been ameliorated the difference between our data and the experimental ones³² that the differences are acceptable ($< 33.68 \text{ cm}^{-1}$ for silver and $< 50 \text{ cm}^{-1}$ for hydrogen) (see the Tables 1 and 2).

We have been used a chain of programs developed in the quantum physics laboratory in Toulouse to investigate the PECs and the dipole moments. This chain is composed of the Toulouse package code (RCUT, PSHF, IJKL, FOCK, CIPSI, CVAL, MOYEN, BDAV...) ³³⁻⁵². The spectroscopic parameters were determined by fitting the vibrational levels with the method of least square. The ionization potential of silver is $61,106.45 \text{ cm}^{-1}$ and the electron affinity of hydrogen is 6083.057 cm^{-1} . The energy of the first ionic limit $\text{Ag}^+ + \text{H}^-$ is equal to $55,023.393 \text{ cm}^{-1}$ (see Table 3).

Adiabatic PEC_s and their spectroscopic parameters. To study the AgH molecule we have been used the P.P approach, which reduces the number of electrons in the molecular system to two valence electrons which allows, thereafter, performing a complete configuration interaction. In this part, we have been displayed the adiabatic results: PECs and spectroscopic constants (R_e : equilibrium distance, D_e : well depth, T_e : excitation energy

Asymptotes	Molecular states	This work (cm ⁻¹)	Exp ³² -PI(cm ⁻¹)	ΔE
Ag (5 s) + H (1 s)	$1,^3\Sigma$	-170,785.2216	-170,785.2216	0.00
Ag (5p) + H (1 s)	$1,^3\Sigma, ^3\Pi$	-140,619.4266	-140,619.4266	0.00
Ag (6 s) + H (1 s)	$1,^3\Sigma$	-128,278.9678	-128,229.0696	49.9
Ag (6p) + H (1 s)	$1,^3\Sigma, ^3\Pi$	-122,365.6628	-122,352.2176	13.45
Ag (5d) + H (1 s)	$1,^3\Sigma, ^3\Pi, ^3\Delta$	-122,029.1026	-122,029.1026	0.00
Ag (7 s) + H (1 s)	$1,^3\Sigma$	-118,939.0058	-118,898.2476	40.76
Ag (7p) + H (1 s)	$1,^3\Sigma, ^3\Pi$	-116,711.5578	-116,690.8056	20.76
Ag (6d) + H (1 s)	$1,^3\Sigma, ^3\Pi, ^3\Delta$	-116,618.4998	-116,575.8316	42.67

Table 3. Various molecular states of AgH below the ionic limit ($\text{Ag}^+ + \text{H}^-$). ΔE Energy difference between the experimental values and theoretical work in cm⁻¹.

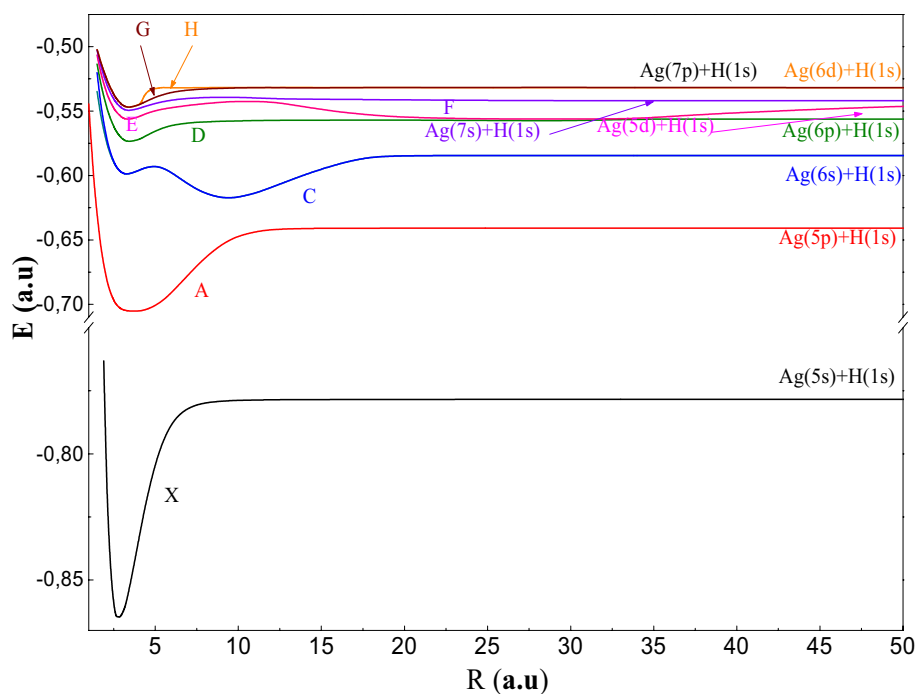


Figure 1. Potential energy curves of the $1\Sigma^+$ states of AgH molecule.

vertical, ω_e : the pulsation at equilibrium, $\omega_e\chi_e$: the constant of anharmonicity and B_e : the constant rotational) of the 30 electronic states $1,^3\Sigma^+$, $1,^3\Pi$ and $1,^3\Delta$ symmetries tends to the ionic limit ($\text{Ag}^+ + \text{H}^-$). In Figs. 1, 2, 3, 4, 5, we have been drawn these curves for a huge grid of points from 1.5 to 200 a.u. In Table 4, we have been displayed the spectroscopic parameters states' with the available theoretical work.

In Fig. 1, we present the adiabatic PECs of the states of $1\Sigma^+$ symmetry of the AgH molecule over the internuclear distance interval R between 1.5 a.u. and 50 a.u. We can see in this figure that the ground state $X^1\Sigma^+$ dissociates towards their asymptotic limit ($\text{Ag}(5s) + \text{H}(1s)$) and has a single deep well ($D_e = 19,100 \text{ cm}^{-1}$), which is near of reference¹ ($D_e = 19,250 \pm 200 \text{ cm}^{-1}$). Our equilibrium distance is of the order of 2.91 a.u., which is near to the equilibrium distance $R_e = 2.95 \text{ a.u.}$ ⁵. Moreover, our pulsation ω_e is equal to 1606 cm^{-1} and our anharmonicity constant $\omega_e\chi_e = 27 \text{ cm}^{-1}$ are near to that obtained by Witek et al.¹⁴ ($= 1759.9 \text{ cm}^{-1}$ and $\omega_e\chi_e = 34.06 \text{ cm}^{-1}$). Turn on the first excited $A^1\Sigma^+$ state, which dissociates towards $\text{Ag}(5p) + \text{H}(1s)$ has a wider well ($D_e = 17,989 \text{ cm}^{-1}$) at $R_e = 3.35 \text{ a.u.}$ Then, the second excited state $C^1\Sigma^+$ tends rapidly towards their dissociation limit ($\text{Ag}(6s) + \text{H}(1s)$) at the distance 25 a.u. Indeed, $C^1\Sigma^+$ have double well, the first well is of depth 3154 cm^{-1} at $R_e = 3.32 \text{ a.u.}$ and the second is of depth 7233 cm^{-1} at $R_e = 9.45 \text{ a.u.}$ We present in Table 4a the comparison of our spectroscopic parameters with that available in the literature^{5, 6, 8, 12-14} for the states of $X^1\Sigma^+$ and $A^1\Sigma^+$. We notice that the difference between the well depth of $X^1\Sigma^+$ for Le Roy et al.⁵, Seto et al.⁶ and Witek et al.¹² is of the order of 2000 cm^{-1} . On the other hand, the difference between our well depth and those for Le Roy et al.⁵ and Seto et al.⁶ is of the order of 150 cm^{-1} . Concerning the equilibrium distance, the difference between our result and that for Witek et al.¹⁴ is equal to 0.04 a.u. In addition, the comparison between our results of $A^1\Sigma^+$ and that in the literature is in good accordance (see Table 4a). The PECs of the higher excited states of symmetry sigma singlets denoted

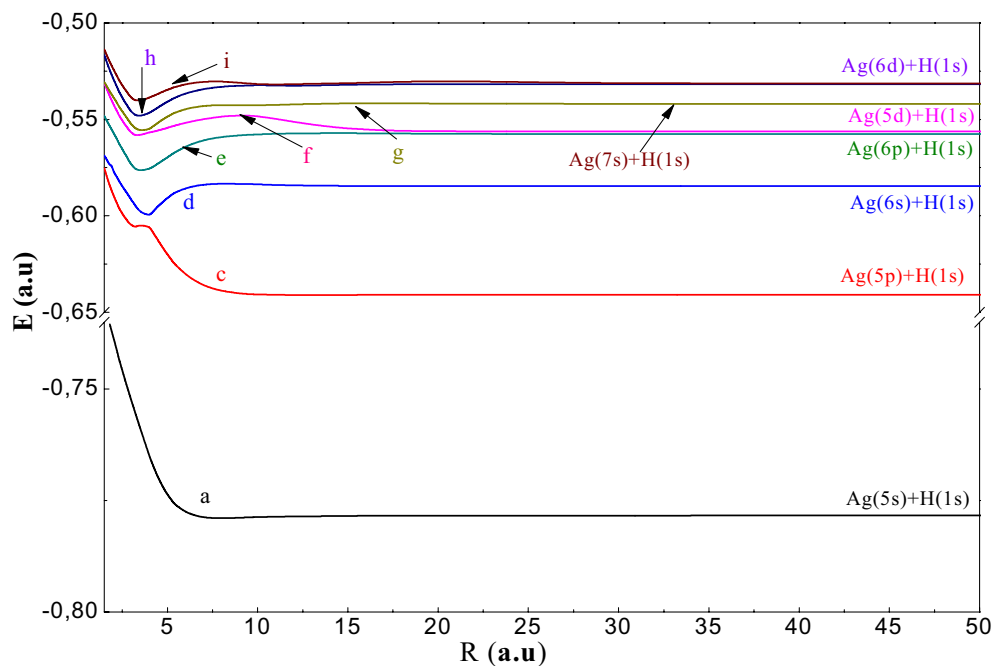


Figure 2. Potential energy curves of the $^3\Sigma^+$ states of AgH molecule.

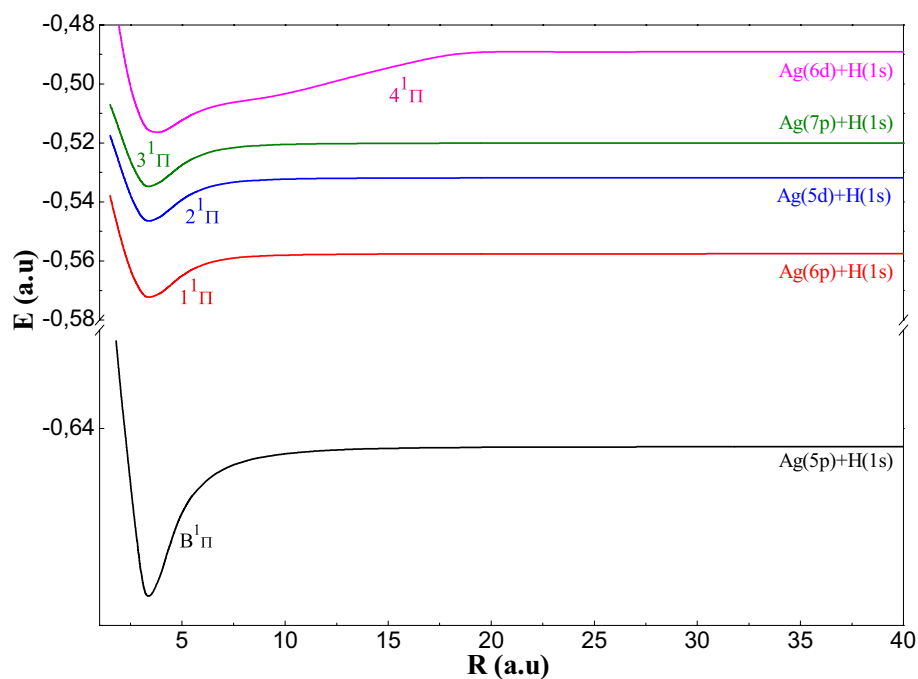


Figure 3. Potential energy curves of the $^1\Pi$ states of AgH molecule.

D; E; F; G and H are presented in the same Fig. 1. All of these states are attractive and their well depths are not deep. We observe the existence of the avoided crossings between the states of the same nature (neutral–neutral) at short distance [(D $^1\Sigma^+$, E $^1\Sigma^+$) and (E $^1\Sigma^+$, F $^1\Sigma^+$)] and ionic neutral [(X $^1\Sigma^+$, A $^1\Sigma^+$), (A $^1\Sigma^+$, C $^1\Sigma^+$) and (C $^1\Sigma^+$, D $^1\Sigma^+$)] (see Table 5). These crossings become less and less avoided, and the difference of energy at these positions becomes smaller at long distances. Their spectroscopic parameters are given in Table 4, which are determined for the first time.

We have been presented in Fig. 2, the adiabatic potential energy curves of the triplet sigma states $^3\Sigma^+$. We notice that a $^3\Sigma^+$ and c $^3\Sigma^+$ are almost repulsive because of the lack of interaction with the ionic curve except for the

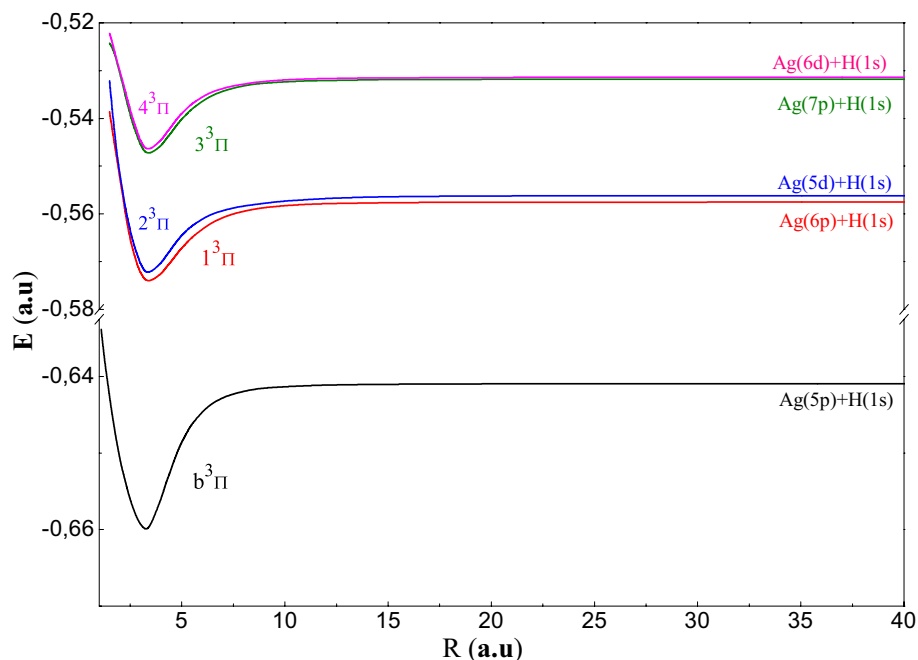


Figure 4. Potential energy curves of the $^3\Pi$ states of AgH molecule.

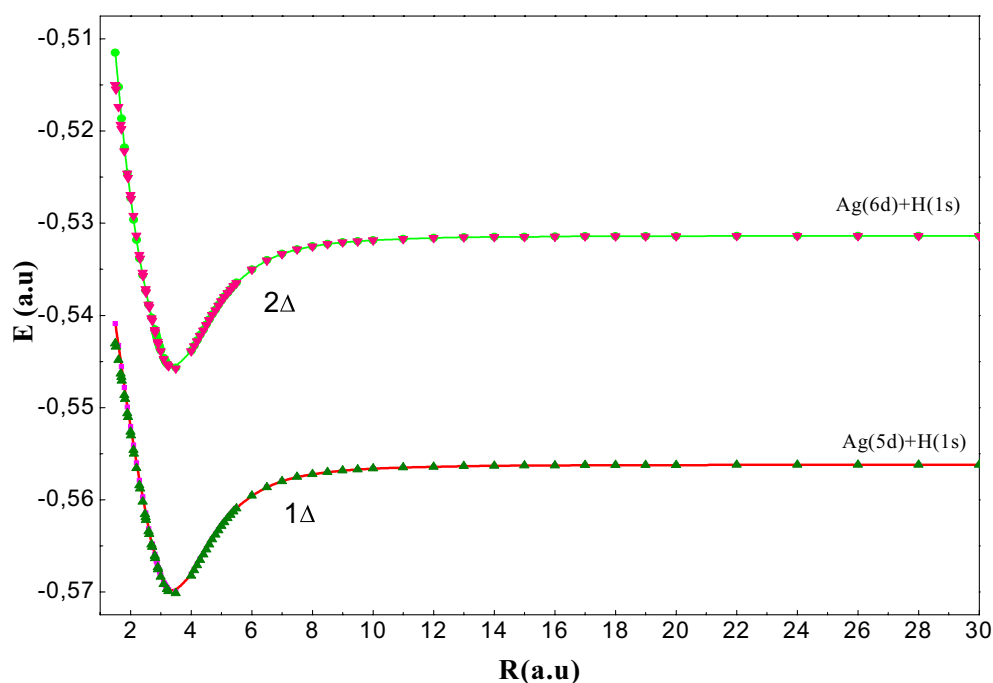


Figure 5. Potential energy curves of the $^1\Delta$ (symbol) and $^3\Delta$ (continuous line) states of AgH molecule.

state d, e and h which present a shallow well of values 3494, 4208 and 3629 cm^{-1} , respectively. The spectroscopic parameters of these states are given in Table 4b.

We have been displayed in Figs. 3 and 4, the PECs related respectively to the $^1,^3\Pi$ symmetry states. These curves relating to these states have a regular shape. Indeed, all the curves have a single minimum of potential and tend quickly (≈ 15 a.u.) towards their asymptotic limit except of state $4^1\Pi$. The triplet states $^3\Pi$ are deeper than the singlet ones ($D_e > 1700$ cm^{-1} for $^1\Pi$ and $D_e > 3336$ cm^{-1} for $^3\Pi$). The spectroscopic parameters of the $^1,^3\Pi$ states are given in Table 4c. We notice that in Fig. 4 that the states ($1^3\Pi$, $2^3\Pi$) and ($3^3\Pi$, $4^3\Pi$) have avoided crossings between them.

States	R_e (a.u.)	D_e (cm ⁻¹)	T_e (cm ⁻¹)	ω_e (cm ⁻¹)	$\omega_e x_e$ (cm ⁻¹)	B_e (cm ⁻¹)	References
(a) $^1\Sigma^+$ states							
$X^1\Sigma^+$	2.91	19,100	0	1606	27	7.7	This work
	3.05	19,250 (± 200)	0	–	–	–	le Roy ⁵
	3.04	19,300	–	–	–	–	Seto ⁶
	3.05	21,200	0	1759.9	34.06	6.45	Witek ¹²
	3.04	–	0	1819	80	6.36	Li ¹³
	2.95	20,387	–	2073	52.7	6.904	Witek ¹⁴
	3.06	–	–	1760	–	6.43	Brike et al. ⁸
$A^1\Sigma^+$	3.35	17,989	35,634	1376	28	4.38	This work
	3.11	18,830.646	29,971	–	–	–	le Roy ⁵
	3.15	19,100	29,959	1663.6	87	6.265	Witek ¹²
	3.09	–	30,321	–	–	6.17	Li ¹³
	3.24	18,544	32,208	1422	27.3	5.730	Witek ¹⁴
	3.03	–	–	1805	–	6.56	Brike et al. ⁸
$C^1\Sigma^+$	3.32	3154	58,968	–	2.63	5.47	This work
2nd min	9.45	7233	–	303	–	0.68	
$D^1\Sigma^+$	3.32	3154	58,999	1665	75	5.47	
2nd min	9.44	7233	–	–	–	–	
$E^1\Sigma^+$	3.5	3852	64,958	719	36	4.92	
$F^1\Sigma^+$	3.4	3178	68,443	23	0.74	5.2	
(b) $^3\Sigma^+$ states							
$a^3\Sigma^+$	7.87	121	57,404	75	12	0.97	This work
$c^3\Sigma^+$	3.21	22	60,476	17	3.62	5.85	
$d^3\Sigma^+$	3.85	3494	64,517	929	61.26	4.07	
$e^3\Sigma^+$	3.58	4208	67,987	628	23.09	4.7	
$f^3\Sigma^+$	3.36	457	68,787	564	22.06	5.34	
2 nd min	27.6	3	–	–	–	0.079	
$g^3\Sigma^+$	3.64	3108	69,007	708	40.63	4.55	
$h^3\Sigma^+$	3.48	3629	70,458	617	26.78	4.98	
$i^3\Sigma^+$	3.41	1990	71,983	653	52.05	5.18	
(c) $^1,^3\Pi$ states							
$B^1\Pi$	3.42	1700	35,756	422	27.81	5.15	This work
$b^3\Pi$	3.21	4244	45,210	651	24.92	5.85	
$1^1\Pi$	3.46	3282	65,094	660	33.75	5.04	
$1^3\Pi$	3.45	3647	64,594	583	23.73	5.06	
$2^1\Pi$	3.45	3269	70,706	610	28.8	5.06	
$2^3\Pi$	3.42	3546	65,061	558	23.07	5.15	
$3^1\Pi$	3.44	3278	73,269	624	30.17	5.09	
$3^3\Pi$	3.45	3437	70,502	599	26.56	5.06	
$4^1\Pi$	3.73	6093	78,205	346	7.87	4.33	
$4^3\Pi$	3.43	3336	70,693	600	27.7	5.12	
(d) $^1,^3\Delta$ States							
$1^1\Delta$	3.43	3197	65,500	700	38.49	5.12	This work
$1^3\Delta$	3.42	3069	65,456	631	32.28	5.15	
$2^1\Delta$	3.43	3030	70,862	570	26.26	5.12	
$2^3\Delta$	3.43	3169	70,840	634	31.65	5.12	
$3^1\Delta$	3.43	3155	73,329	609	29.6	5.12	
$3^3\Delta$	3.44	3205	73,318	634	31.42	5.09	

Table 4. Spectroscopic constants for $^1,^3\Sigma^+$, $^1,^3\Pi$ and $^1,^3\Delta$ states of AgH.

States	X/A	A/C	C/D	D/E	E/F	F/G	G/H
Positions (a.u)	5	9	17	34	35	64	181.6

Table 5. Avoided crossing positions.

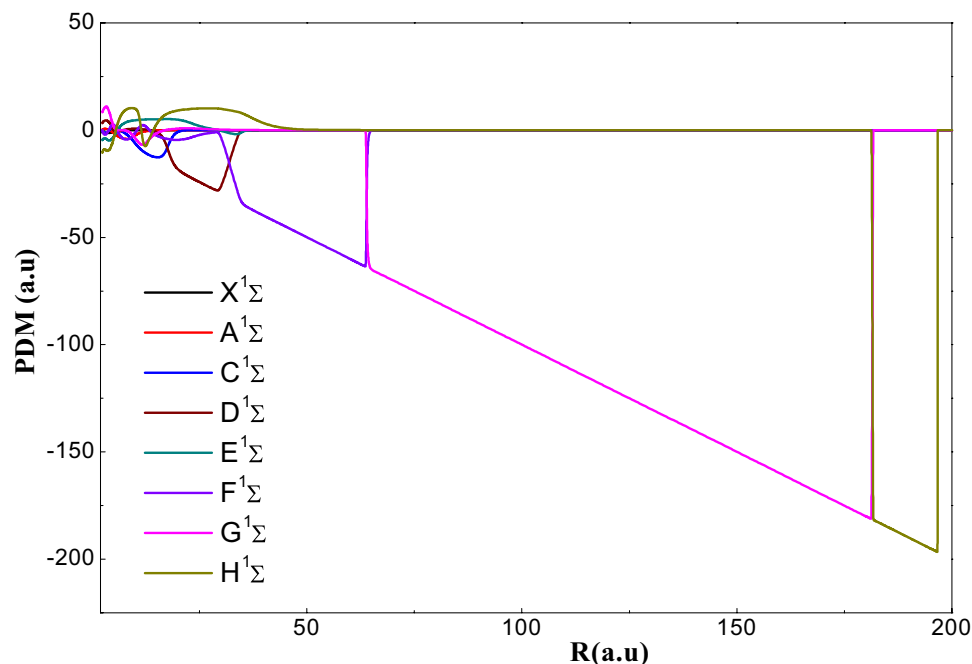


Figure 6. Permanent dipole moment for the $1\Sigma^+$ states for the AgH molecule.

We have been studied four states of delta $4^{1,3}\Delta$ symmetry. The PECs related to the $4^{1,3}\Delta$ states are drawn respectively in Fig. 5. These curves have regular shapes with one minimum potential of the order of 3.43 a.u. Moreover, the triplets and singlets $1^3\Delta$ dissociating towards the same limit are quasi-degenerate which is confirmed by the results in Table 4d.

Electronic dipole moment properties of AgH. In Fig. 6, we have been displayed the curves of the permanent dipole moments PDM of (1–8) $1\Sigma^+$ of AgH. We can see that all the curves has a linear part and all of these linear form are segments of the identical line of slope $(-R)$. We can see that the junction between two linear forms belonging to two successive states $1\Sigma^+$ corresponding to an avoided crossing between the states. Therefore, that at the avoided crossing there is a sudden variation in the permanent dipole moment, and this inter-nuclear distance becomes bigger. On the other hand, that the dipole moment variation at short range is very smooth. There are slow variations at short inter-nuclear distance although this variation is sharp for large distances (see Figure S1.a and b).

The curves of the PDM of the 8 triplet sigma states $3\Sigma^+$ are shown in Fig. 7 whose the inter-nuclear distance varies from 2 to 60 (a.u.). From this figure, we can observe that there is no abrupt variation and there is no line segments associated with the ionic character as in symmetry $3\Sigma^+$. The analysis of these curves shows the presence of short-distance extreme, which is explained by the transfer of charges between neutral states. This justifies the absence of the ionic curve. We can observe in Figure S2 that the crossings of the PDM variation curves from 1Π states for $R = 9$ a.u. and $R = 18$ a.u. related to the positions of the avoided crossings (P.A.C). Whereas, for the short distance, the variation is slight and for the long distance this variation is abrupt. We can see that the curves of the singlet states are identical to those of the triplet states that confirm the shapes of the PECs (see Figure S3).

Move on for the transition dipole moment curves, we observe in Fig. 7a,b that the variations are slight and the extremes coincide at the P_{AC} in the PECs for example, the X-A transitions at a maximum of the order of 5 a.u. and the C-D transitions at a maximum of the order of 4.5 a.u. So, we can conclude that these extremes are characterized by the maximum of ionic character. The observation of Fig. 8 shows that the variations are slight as the curves of the TDMs correspond to $1\Sigma^+$ symmetry and the maximum of TDM ($2^1\Pi-3^1\Pi$) is located at $R = 5.2$ a.u. corresponding to the P.A.C. in the potential energy curves. Examining the Fig. 9, we find that these transitions of $1^3\Delta$ have slight variations; passing through a single extreme corresponding to the maximum of ionic character.

Vibrational levels of AgH. After determining of the dipole moments, we have been investigated the vibrational levels of 30 electronic states as well as their spacing's. The analysis of the vibrational levels of different electronic states is of great importance. Indeed, the spacing between these vibration levels provides precise information on the shapes of the PECs as indicated in reference³⁵.

In Fig. 10, we have been illustrated the spacing's between the vibrational levels of the ground state $X^1\Sigma^+$. Note that the spacing's are not constant, which is reflected the anharmonicity of the well. At the beginning, the variation is linear decreasing which related to the regular anharmonic shape of the PECs (see Fig. 10a) then it is constant and attains the dissociation limit $Ag(5p) + H(1s)$ (see Fig. 10b). This behavior is similar to the ground state spacing of BaH^+ ³⁵ and $X^2\Sigma^+$ barium hydride from $BaXe$ ³⁶. The observation of the state $C^1\Sigma^+$ indicate the

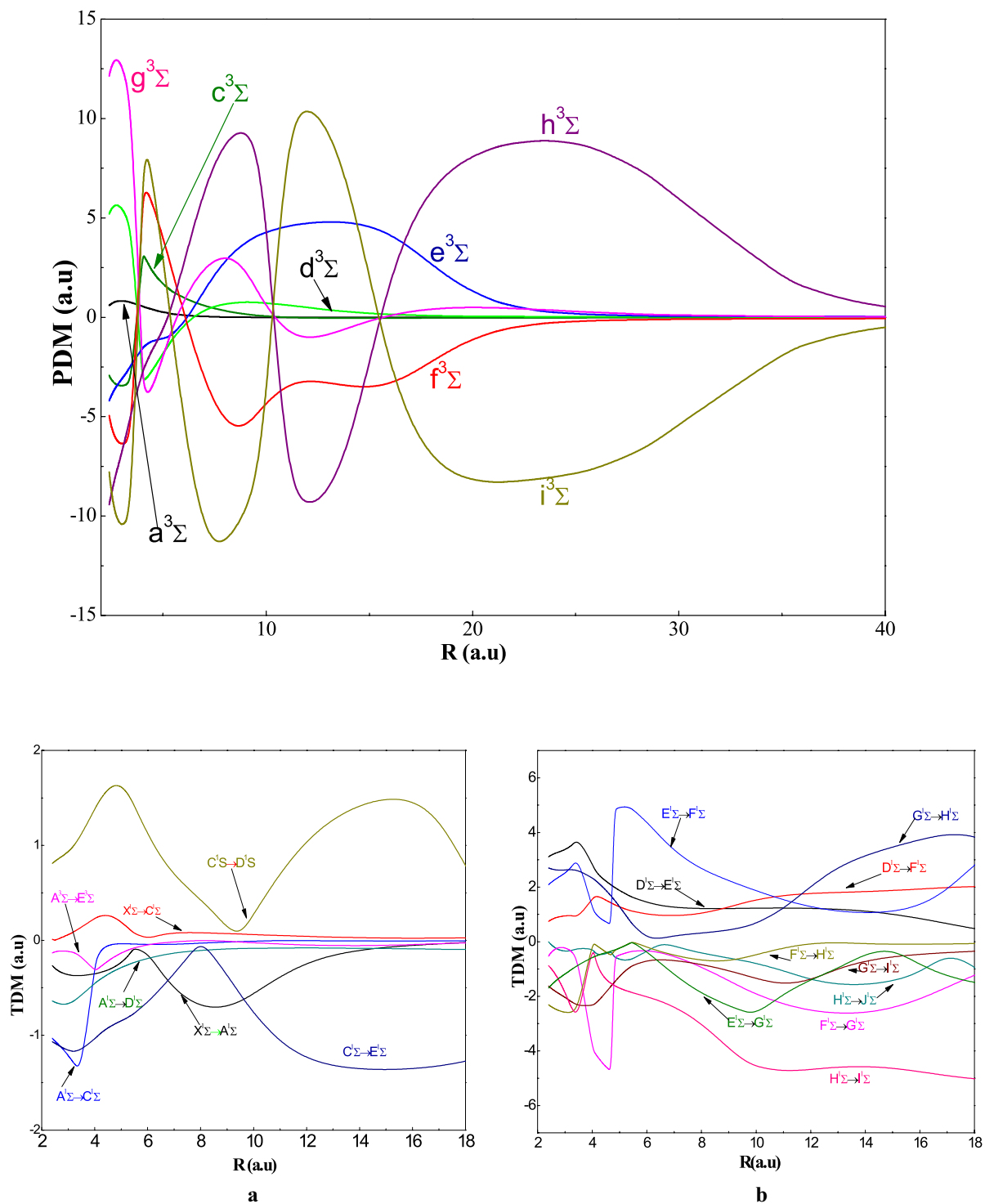


Figure 7. Permanent dipole moment for the $3\Sigma^+$ states for the AgH molecule. (a) Transition Dipole Moment from the states $i=1, 2$ et 3 to the states $j=i+1, i+2$ of the symmetry 1Σ of AgH molecule. (b) Transition Dipole Moment from the states $i=4, 5, 6, 7$ et 8 to the states $j=i+1, i+2$ of the symmetry 1Σ of AgH molecule.

variation of the curve of spacing's between levels is almost linear and decreasing until $v=17$ and we have a degenerate level $v=18$ therefore the appearance of a second well smaller than the other. Then, from $v=27$ to $v=40$, we observe a significant drop which reflects the presence of very numerous and tight spaces near to the limit. Move on to the $D^1\Sigma^+$, we can see the shape of the well is regular anharmonic up to $v=10$ as a result of a sudden change of pace which translates an important and rapid widening, from $v=10$, the levels become tight and numerous.

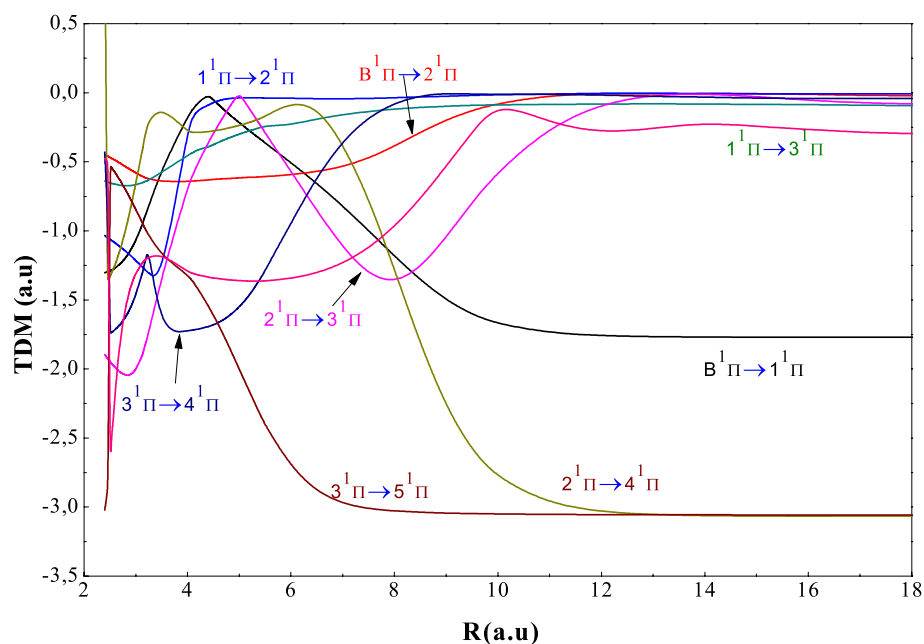


Figure 8. Transition dipole moment for the $^1\Pi$ states for the AgH molecule.

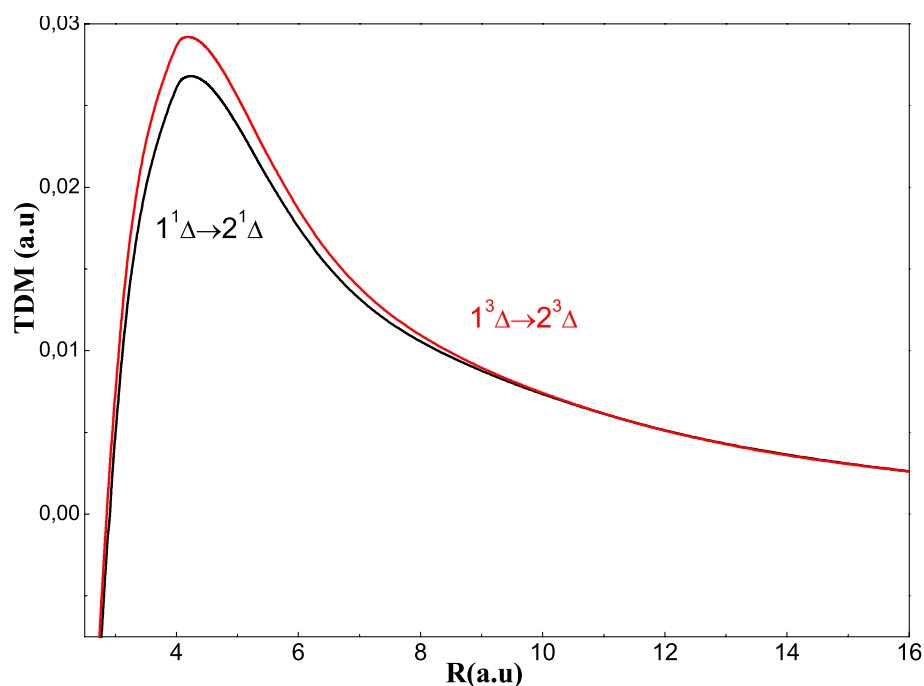


Figure 9. Transition dipole moment for the $^1\Delta$ states for the AgH molecule.

Conclusion

We have been started this work by building and optimizing the bases to reproduce the transition energy spectra of silver atoms and hydrogen. Next, we have been calculated the adiabatic PECs of 30 molecular states ($16\ ^1\Sigma^+$, $10\ ^1\Sigma^-$, and $4\ ^1\Delta$) lying to the $\text{Ag}^+ + \text{H}^-$ asymptotic limit. Then, we have been calculated the spectroscopic parameters (D_e , R_e , T_e , ω_e , χ_e , ω_c and B_e) from these curves. We compared our study with experimental and theoretical ones available in the literature^{6–25}. We observe a good accordance with the experimental and theoretical data, which builds a validation criterion for our method.

We have been determined the vibration levels of each electronic state as well as their spacing's. Analysis of these properties gives precise information about the shape of the PECs. Moreover, we have been investigated

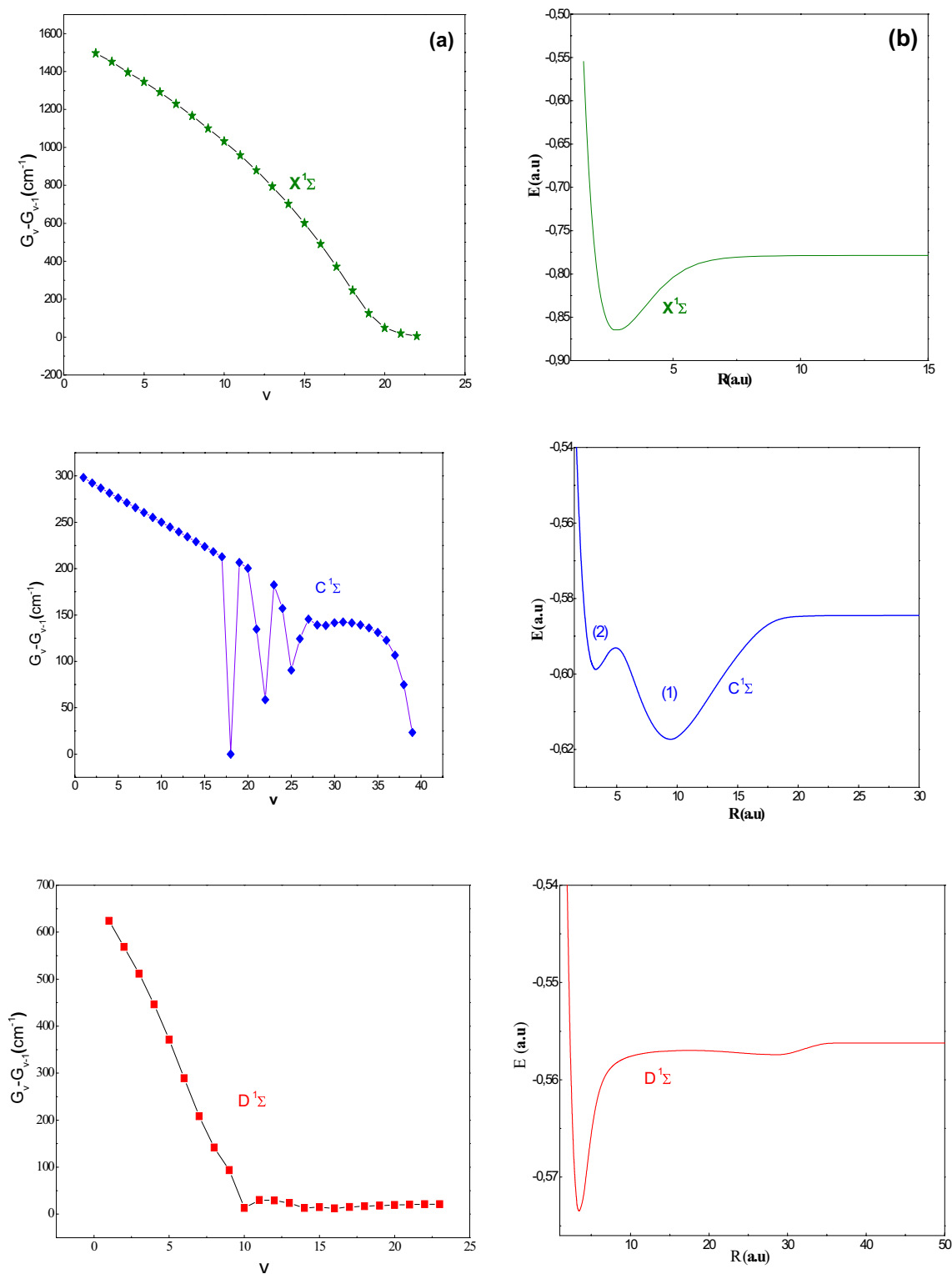


Figure 10. Vibrational spacing (left) and potential energy curves (right) for (X, C and D) ¹Σ⁺ states of AgH.

the electrical dipolar properties (PDM, TDM), which make it possible to confirm that the ionic character for the AgH molecule is in the ¹Σ⁺ symmetry.

Received: 8 December 2020; Accepted: 26 March 2021
Published online: 15 April 2021

References

1. Evgeny, L., Houhua, L. & Clément, M. Well-defined transition metal hydrides in catalytic isomerizations. *Chem. Commun.* **50**(69), 9816–9826 (2014).
2. Tianfei, L. *et al.* Accelerating proton-coupled electron transfer of metal hydrides in catalyst model reactions. *Nat. Chem.* **10**, 881–887 (2018).
3. Abdullah, C. & Mustafa, K. Electronic structure, elastic and phonon properties of perovskite-type hydrides $MgXH_3$ ($X = Fe, Co$) for hydrogen storage. *Solid State Commun.* **281**, 38–43 (2018).
4. Langhoff, S. R., Pettersson, L. G. M., Bauschlicher, C. W. Jr. & Partridge, H. Theoretical spectroscopic parameters for the low-lying states of the second-row transition metal hydrides. *J. Chem. Phys.* **68**, 278–286 (1987).
5. Le Roy, R. J., Appadoo, D. R. T., Anderson, K. & Shayesteh, A. Direct-potential-fit analysis of new infrared and UV/visible $A^1\Sigma^+ - X^1\Sigma^+$ emission spectra of AgH and AgD. *J. Chem. Phys.* **123**, 204304 (2005).
6. Seto, J. Y. *et al.* Vibration-rotation emission spectra and combined isotopomer analyses for the coinage metal hydrides: CuH & CuD, AgH & AgD, and AuH & AuD. *J. Chem. Phys.* **110**, 11756 (1999).
7. Rolf-Dieter, U., Birk, H., Polomsky, P. & Jones, H. The ground state infrared spectra of four diatomic deuterides (GaD, InD, TlD, AgD) and the determination of mass-independent molecular parameters. *J. Chem. Phys.* **94**, 4 (1991).
8. Brike, H. & Jones, H. The ground state infrared spectra of two isotopic forms of silver hydride (^{107}AgH and ^{109}AgH). *Chem. Phys. Lett.* **161**, 1 (1989).
9. Holden, S. J. & Rossington, D. R. Hydrogen adsorption on silver, gold, and aluminum. Studies of parahydrogen conversion. *J. Phys. Chem.* **68**, 1061 (1964).
10. Souissi, H. & Mohamed, B. Y. Application of innovative analytical modeling for the physicochemical analysis of adsorption isotherms of silver nitrate on helicenes: Phenomenological study of the complexation process. *Adsorp. Sci. Technol. Article ID 6619389*, 14 (2021).
11. Manel, B. Y. & Mohamed, B. Y. Physico-chemical study of complexation of silver ion (Ag^+) by macrocyclic molecules (hexa-Helicenes) based on statistical physics theory: New description of a cancer drug. *Sci. Rep.* **10**, 10328 (2020).
12. Witek, H. A., Nakajima, T. & Hirao, K. Relativistic and correlated all-electron calculations on the ground and excited states of AgH and AuH. *J. Chem. Phys.* **113**, 8015 (2000).
13. Li, Y., Libermann, H. P., Buenker, R. J. & Pichl, L. A coupled treatment of $^1\Sigma^+$ and $^3\Pi$ states of AgH molecule. *Chem. Phys. Lett.* **389**, 101 (2004).
14. Witek, H. A., Fedorov, D. G., Hirao, K., Viel, A. & Widmark, P. O. Theoretical study of the unusual potential energy curve of the $A^1\Sigma^+ - X^1\Sigma^+$ state of AgH. *J. Chem. Phys.* **116**, 8396 (2002).
15. Richard Martin L., All-Electron Relativistic Calculations on AgH. An Investigation of the Cowan-Griffin Operator in a Molecular Species. *J. Phys. Chem.* **87**, 750–754 (1983).
16. Robert Le Roy, J. & Huang, Y. Representing Born-Oppenheimer breakdown radial correction functions for diatomic molecules. *J. Mol. Struct. (Theochem)* **591**, 175–187 (2002).
17. Mohanty, A. K. & Parpia, F. A. Fully relativistic calculations for the ground state of the AgH molecule. *Phys. Rev. A* **54**, 4 (1996).
18. Jenning, S. Y. *et al.* Vibration-rotation emission spectra and combined isotopomer analyses for the coinage metal hydrides: CuH & CuD, AgH & AgD, and AuH & AuD. *J. Chem. Phys.* **110**, 24 (1999).
19. Liu, C. W. *et al.* Stable silver(I) hydride complexes supported by diseleno-phosphate ligands. *Inorg. Chem.* **49**, 468–475 (2010).
20. Hess, B. A. & Chandra, P. Relativistic *ab initio* CI study of the $X^1\Sigma^+$ and $A^1\Sigma^+$ states of the AgH molecule. *Phys. Script.* **36**, 412–415 (1987).
21. Andrews, L. & Wang, X. Infrared spectra and structures of the stable CuH_2^- , AgH_2^- , AuH_2^- , and AuH_4^- anions and the AuH₂ molecule. *J. Am. Chem. Soc.* **125**, 11751–11760 (2003).
22. Xie, H. *et al.* Probing the structural and electronic properties of Ag_nH^- ($n = 1-3$) using photoelectron imaging and theoretical calculations. *J. Chem. Phys.* **136**, 184312 (2012).
23. Charlene, C. L., Kenneth, D. G. & Henry, S. F. Relativistic and correlation effects in CuH, AgH, and AuH: Comparison of various relativistic methods. *J. Chem. Phys.* **102**, 2024 (1995).
24. Richard, R. B. & Walter, E. C. *Ab initio* calculations including relativistic effects for Ag^2 , Au^2 , $AgAu$, AgH , and AuH . *J. Phys. Chem.* **89**, 24 (1985).
25. Stoll, H. *et al.* Cu and Ag as one-valence-electron atoms: CI results and quadrupole corrections for Cu₂, Ag₂, CuH, and AgH. *J. Chem. Phys.* **79**, 5532 (1983).
26. Bengtsson, E. & Olsson, E. Eine neue Untersuchung über die Banden des Silberhydrides. *Z. Phys.* **72**, 163 (1931).
27. Durand, Ph. & Barthelat, J. C. A theoretical method to determine atomic pseudopotentials for electronic structure calculations of molecules and solids. *Theor. Chim. Acta* **38**, 283 (1975).
28. Durand, Ph. & Barthelat, J. C. New atomic pseudopotentials for electronic structure calculations of molecules and solids. *Chem. Phys. Lett.* **27**, 191–194 (1974).
29. Müller, W., Flesh, J. & Meyer, W. Treatment of intershell correlation effects in *ab initio* calculations by use of core polarization potentials. Method and application to alkali and alkaline earth atoms. *J. Chem. Phys.* **80**, 3297 (1984).
30. Foucrault, M. & Millie, P. Nonperturbative method for core-valence correlation in pseudopotential calculations: Application to the Rb₂ and Cs₂ molecules. *J. Chem. Phys.* **96**, 1257 (1992).
31. Zrafi, W., Oujia, B. & Gadea, F. X. Theoretical study of the CsH molecule: adiabatic and diabatic potential energy curves and dipole moments. *J. Phys. B: At. Mol. Opt. Phys.* **39**, 3815 (2006).
32. Ralchenko, Y., Kramida, A., Reader, J., NIST ASD Team 2011 NIST Atomic Spectra Database (version 4.1). Available at: <http://physics.nist.gov/asd/>.
33. Gaied, W., Habli, H., Oujia, B. & Gadea, F. X. Theoretical study of the MgAr molecule and its ion Mg^+Ar : Potential energy curves and spectroscopic constants. *J. Eur. Phys.* **62**, 371 (2011).
34. Gaied, W. & Oujia, B. Potential energy curves, permanent and transition dipole moments for numerous electronic excited states of CaAr. *Int. J. Nanoparticles* **3**, 160 (2010).
35. Mejrissi, L., Habli, H., Ghalla, H., Oujia, B. & Gadea, F. X. Adiabatic *ab initio* study of the BaH⁺ ion including high energy excited states. *J. Phys. Chem. A* **117**, 5503 (2013).
36. Abdesslem, K., Mejrissi, L., Issaoui, N., Oujia, B. & Gadéa, F. X. One and two-electron investigation of electronic structure for Ba⁺Xe and BaXe van der Waals molecules in a pseudopotential approach. *J. Chem. Phys.* **36**(117), 8925–8938 (2013).
37. Habli, H., Ghalla, H., Oujia, B. & Gadea, F. X. *Ab initio* study of spectroscopic properties of the calcium hydride molecular ion. *Eur. Phys. J. D* **64**, 5 (2011).
38. Habli, H., Dardouri, R., Oujia, B. & Gadéa, F. X. *Ab initio* adiabatic and diabatic energies and dipole moments of the CaH⁺ molecular ion. *J. Chem. Phys.* **115**, 14045–14053 (2011).
39. Chaieb, M., Habli, H., Mejrissi, L., Oujia, B. & Gadea, F. X. *Ab initio* spectroscopic study for the NaRb molecule in ground and excited states. *J. Quantum Chem.* **114**, 731–747 (2014).
40. Habli, H. *et al.* *Ab initio* calculation of the electronic structure of the strontium hydride ion (SrH^+). *Int. J. Quantum Chem.* **115**, 172–186 (2015).

41. Guérout, R., Aymar, M. & Dulieu, O. Ground state of the polar alkali-metal-atom–strontium molecules: Potential energy curve and permanent dipole moment. *Phys. Rev. A* **82**, 042508 (2010).
42. Dardouri, R., Issa, K., Oujia, B. & Gadéa, F. Xavier, Theoretical study of the electronic structure of LiX and NaX (X = Rb, Cs) molecules. *Int. J. Quant. Chem.* **112**, 2724–2734 (2012).
43. Dardouri, R., Habli, H., Oujia, B. & Gadéa, F. X. Theoretical study of the electronic structure of KLi molecule: Adiabatic and diabatic potential energy curves and dipole moments. *Chem. Phys.* **399**, 65–79 (2012).
44. Khémiri, N., Dardouri, R., Oujia, B. & Gadea, F. X. Ab initio investigation of electronic properties of the magnesium hydride molecular ion. *J. Phys. Chem. A* **117**, 8915–8924 (2013).
45. Khelifi, N., Oujia, B. & Gadea, F. X. Dynamic couplings, radiative and nonradiative lifetimes of the $A^1\Sigma^+$ and $C^1\Sigma^+$ states of the KH molecule. *J. Phys. Chem. Ref. Data* **36**, 191–202 (2007).
46. Dardouri, R., Habli, H., Oujia, B. & Gadéa, F. X. Ab Initio Diabatic energies and dipole moments of the electronic states of RbLi molecule. *J. Comp. Chem.* **34**, 2091–2099 (2013).
47. Habli, H. *et al.* Ab initio investigation of the electronic and vibrational properties for the $(CaLi)^+$ ionic molecule. *Mol. Phys.* **114**, 1568–1582 (2016).
48. Souissi, H. *et al.* Spectroscopic ab initio investigation of the electronic properties of $(SrK)^+$. *Chem. Phys.* **490**, 19–28 (2017).
49. Souissi, H. *et al.* An adiabatic spectroscopic investigation of the CsRb system in ground and numerous excited states. *J. Qu. Spect. Rad. Tran.* **200**, 173–189 (2017).
50. Mtiri, S. *et al.* Theoretical investigation of the diatomic Van der Waals systems Ca^+He and $CaHe$. *Comput. Theo. Chem.* **1114**(15), 33–46 (2017).
51. Hamdi, R. *et al.* Spectroscopic and electric dipole properties of Sr^+Ar and $SrAr$ systems including high excited states. *J. Phys. B At. Mol. Opt. Phys.* **51**, 025004 (2017).
52. Souissi, H. *et al.* Ab initio diabatic and adiabatic calculations for francium hydride FrH . *J. N. Chem.* **44**(14), 5572–5587 (2020).

Acknowledgments

This research was funded by the Deanship of Scientific Research at Princess Nourah Bint Abdulrahman University through the research The Fast-track Research Funding Program.

Author contributions

T.A.A. and H.S. wrote the main manuscript text and F.H.A. and F.A. prepared all figures. Then, all authors reviewed the manuscript.

Competing interests

The authors declare no competing interests.

Additional information

Supplementary Information The online version contains supplementary material available at <https://doi.org/10.1038/s41598-021-87433-2>.

Correspondence and requests for materials should be addressed to H.S.

Reprints and permissions information is available at www.nature.com/reprints.

Publisher's note Springer Nature remains neutral with regard to jurisdictional claims in published maps and institutional affiliations.



Open Access This article is licensed under a Creative Commons Attribution 4.0 International License, which permits use, sharing, adaptation, distribution and reproduction in any medium or format, as long as you give appropriate credit to the original author(s) and the source, provide a link to the Creative Commons licence, and indicate if changes were made. The images or other third party material in this article are included in the article's Creative Commons licence, unless indicated otherwise in a credit line to the material. If material is not included in the article's Creative Commons licence and your intended use is not permitted by statutory regulation or exceeds the permitted use, you will need to obtain permission directly from the copyright holder. To view a copy of this licence, visit <http://creativecommons.org/licenses/by/4.0/>.

© The Author(s) 2021